Allosteric Mechanisms in Cytochrome P450 3A4 Studied by High-Pressure Spectroscopy: Pivotal Role of Substrate-Induced Changes in the Accessibility and Degree of Hydration of the Heme Pocket†

Dmitri R. Davydov,*,‡ Bradley J. Baas,§ Stephen G. Sligar,§ and James R. Halpert‡

Department of Pharmacology and Toxicology, The University of Texas Medical Branch, 301 University Boulevard, Galveston, Texas 77555, and Department of Biochemistry and Chemistry, Beckman Institute for Advanced Science and Technology, University of Illinois, Urbana, Illinois 61801

Received November 20, 2006; Revised Manuscript Received April 21, 2007

ABSTRACT: Allosteric mechanisms in human cytochrome P450 3A4 (CYP3A4) in oligomers in solution or monomeric enzyme incorporated into Nanodiscs (CYP3A4ND) were studied by high-pressure spectroscopy. The allosteric substrates 1-pyrenebutanol (1-PB) and testosterone were compared with bromocriptine (BCT), which shows no cooperativity. In both CYP3A4 in solution and CYP3A4ND, we observed a complete pressure-induced high-to-low spin shift at pressures of <3 kbar either in the substrate-free enzyme or in the presence of BCT. In addition, both substrate-free and BCT-bound enzyme revealed a pressure-dependent equilibrium between two states with different barotropic parameters designated R for relaxed and P for pressure-promoted conformations. This pressure-induced conformational transition was also observed in the studies with 1-PB and testosterone. In CYP3A4 oligomers, the transition was accompanied by an important increase in homotropic cooperativity with both substrates. Surprisingly, at high concentrations of allosteric substrates, the amplitude of the spin shift in both CYP3A4 in solution and Nanodiscs was very low, demonstrating that hydrostatic pressure induces neither substrate dissociation nor an increase in the heme pocket hydration in the complexes of the pressure-promoted conformation of CYP3A4 with 1-PB or testosterone. These findings suggest that the mechanisms of interactions of CYP3A4 with 1-PB and testosterone involve an effector-induced transition that displaces a system of conformational equilibria in the enzyme toward the state(s) with decreased solvent accessibility of the active site so that the flux of water into the heme pocket is impeded and the high-spin state of the heme iron is stabilized.

Current advances in studies of substrate interactions of cytochromes P450 by biophysical techniques (*1*−*3*) and recently resolved X-ray structures of microsomal cytochrome P450 species (*4*−*6*) have revealed an important conformational flexibility of cytochromes P450 3A4 (CYP3A4)[1] and 2B4 (CYP2B4). The striking conformational rearrangements exhibited by these versatile drug-metabolizing enzymes are thought to play an important role in the adaptation of the geometry of the active site to a diverse set of substrate structures. Further investigation of the molecular mechanisms and functional consequences of these conformational transitions is needed to develop a detailed understanding of the mechanisms of enzyme function. One of the most interesting questions in this regard is the role of the conformational flexibility in the mechanisms of homo- and heterotropic cooperativity exhibited by CYP3A4, the major human hepatic P450 enzyme, which is responsible for metabolism of a broad range of substrates of pharmacological and toxicological interest.

The prevailing hypothesis about the mechanisms of P450 cooperativity is that these enzymes can accommodate multiple substrate molecules in one large binding pocket (*7*−*9*). It was suggested that the binding of several substrate molecules may be required to attain a productive orientation needed for metabolism. However, recent studies from our and other laboratories suggest that P450 cooperativity represents a true case of allostery involving an effector-induced conformational transition (*2*, *3*, *10*−*12*), which is thought to modulate the accessibility and degree of hydration of the active site of the enzyme (*1*, *12*). In this view, pressure-perturbation studies of the interactions of CYP3A4 with allosteric ligands are a timely approach to gaining further mechanistic insight into active site plasticity as related to allostery.

Perturbation of chemical equilibria by hydrostatic pressure provides a powerful technique for studies of the transitions attributable to changes in hydration of macromolecules, such

† This research was supported by NIH Grants GM54995 (J.R.H.), GM33775 (S.G.S.), and GM31756 (S.G.S.), Center Grant ES06676 (J,R,H,), and Robert A. Welch Foundation Grant H1458 (J.R.H.).

* To whom correspondence should be addressed. E-mail: d.davydov@utmb.edu. Telephone: (409) 772-9658. Fax: (409) 772-9642.

‡ The University of Texas Medical Branch.

§ University of Illinois.

[1] Abbreviations: CYP3A4, cytochrome P450 3A4; Hepes, *N*-(2-hydroxyethyl)piperazine-*N*′-2-ethanesulfonic acid; DTT, dithiothreitol; EDTA, ethylenediaminetetraacetic acid; CYP3A4ND, CYP3A4 incorporated into Nanodiscs; BCT, bromocriptine; 1-PB, 1-pyrenebutanol; HPCD, 2-(hydroxypropyl)-*β*-cyclodextrin; DCVJ, 4-(dicyanovinyl)-julolidine.

10.1021/bi602400y CCC: $37.00 © 2007 American Chemical Society
Published on Web 06/08/2007

as protein−protein, protein−DNA, and protein−ligand interactions (*13*−*18*). This approach is especially valuable for studies of heme proteins, where the presence of the heme chromophore allows the use of various spectroscopic techniques for monitoring the transitions between different states of the enzyme. The first studies of pressure-induced transitions in cytochrome P450 species were performed with bacterial P450cam and P450lin (*19*−*24*). Later studies utilized mammalian microsomal CYP2B4 (*25*−*27*), CYP1A2 (*27*, *28*), P450scc (*29*), and CYP3A4 (*11*, *30*), as well as the heme domain of bacterial P450 BM3 (*30*, *31*) and cytochrome CYP119 from a thermophilic archaea (*32*, *33*).

Application of elevated pressure to ferric cytochrome P450 species induces a displacement of the spin equilibrium toward the low-spin state (*19*, *22*, *26*, *29*, *31*, *34*). A second barotropic process was identified as the conversion of the P450 into the inactive state known as P420 (*22*, *24*−*26*). In the case of P450cam, this P450 → P420 transition starts at rather high pressures, when the spin shift is nearly completed (*22*, *35*). For other cytochromes P450, these two pressure-induced processes take place in overlapping pressure ranges (*23*, *26*, *31*).

The effect of pressure-induced changes on the content of the high-spin form of cytochrome P450 in the presence of substrates reflects two concomitant processes: the dissociation of the enzyme−substrate complex and the changes in the spin equilibrium of both substrate-free and substrate-bound enzyme. Application of advanced methods of spectral analysis to the results of pressure-perturbation experiments performed at different substrate concentrations allowed us to resolve the standard volume changes associated with each of these processes in P450cam, P450 BM3, and CYP2B4 (*31*). The substrate-free states of all three enzymes exhibited similar values of standard volume change in the low-spin to high-spin transition ($\Delta V°_{spin}$ = 21−23 mL/mol), which is consistent with expulsion of one molecule of water per molecule of enzyme. In contrast, the $\Delta V°_{spin}$ of the complexes of P450cam, P450 BM3, and CYP2B4 with the substrates camphor, palmitic acid, and benzphetamine, respectively, revealed important differences among these enzymes. While in the case of P450 BM3 the value of $\Delta V°_{spin}$ remained largely unaltered upon substrate binding, CYP2B4 and P450cam exhibited considerable increases in $\Delta V°_{spin}$ upon formation of the corresponding substrate complex. Similarly, the enzymes exhibited important differences in the standard volume changes of dissociation of the substrate complexes. While increasing hydrostatic pressure caused a dissociation of the complexes of P450cam and P450 BMP with their substrates ($\Delta V°_{diss}$ = −48 and −25 mL/mol, respectively), formation of the complex of CYP2B4 with benzphetamine was slightly promoted by pressure ($\Delta V°_{diss}$ = 8.1 mL/mol).

The pressure-induced P450 → P420 transition in CYP3A4 was characterized in detail in our previous publication (*11*), where we demonstrated the distribution of the pool of the enzyme in oligomers into two stable fractions (conformers) having different susceptibilities to pressure-induced inactivation. The study presented here is focused on analysis of the effect of substrates on the pressure-induced spin transitions in CYP3A4 in oligomers in solution and in a monomeric state of the enzyme incorporated into Nanodiscs. We show here that, unlike other P450 enzymes studied to date, CYP3A4 both in oligomers in solution and in Nanodiscs exhibits a pressure-dependent equilibrium between two conformational states that differ significantly in the barotropic parameters of spin transitions and substrate binding. We also demonstrate a striking difference in the pressure-induced transitions in CYP3A4 observed with the allosteric substrates testosterone and 1-pyrenebutanol (1-PB) as opposed to the nonallosteric substrate bromocriptine. Our observations are consistent with a large-scale conformational transition in CYP3A4, which modifies the dynamics of the protein-bound water involved in spin transitions and substrate binding and is central to the mechanism of the cooperativity observed in this enzyme.

MATERIALS AND METHODS

Materials. Bromocriptine (BCT) mesylate, 2-hydroxypropyl-β-cyclodextrin (HPCD), and water-soluble testosterone (HPCD-encapsulated testosterone) were the products of Sigma Chemicals (St. Louis, MO). 1-Pyrenebutanol (1-PB) and 4-(dicyanovinyl)julolidine (DCVJ) were from Invitrogen/Molecular Probes Inc. (Eugene, OR). All other chemicals were ACS grade and were used without further purification.

Expression and Purification of CYP3A4. Wild-type CYP3A4 was expressed as a His-tagged protein in *Escherichia coli* TOPP3 cells and purified as described previously (*2*).

Preparation of Nanodiscs Containing CYP3A4. Soluble nanoscale membrane bilayer particles (Nanodiscs) containing CYP3A4 were obtained by a detergent-removal technique from the mixture of CYP3A4, phospholipid, and a membrane scaffold protein (MSP1D1) as previously described (*36*). Control experiments showed that the Nanodiscs were stable at hydrostatic pressures up to 4.8 kbar (see the Supporting Information).

Experimental. High-pressure spectroscopic studies were performed using a rapid scanning multichannel MC2000-2 spectrophotometer (Ocean Optics, Inc., Dunedin, FL) equipped with an L7893 UV−vis fiber light source (Hamamatsu Photonics K.K.). The instrument was connected by a flexible optic cable to the high-pressure cell (*20*) connected to a manual pressure generator capable of generating a pressure of 6000 bar. All experiments were carried out at 25 °C in 100 mM Na-Hepes buffer (pH 7.4) containing 1 mM DTT and 1 mM EDTA. This buffer is known to be appropriate for pressure-perturbation experiments, as it exhibits a pressure-induced pH change of only −0.06 pH unit/kbar (*25*).

BCT was used in the form of a 300 μM solution in 20 mM sodium acetate buffer (pH 4.0). Control measurements showed that the change in the pH of our samples due to addition of an acidic solution of BCT did not exceed 0.1 pH unit.

1-PB and testosterone were used as complexes with HPCD to diminish pressure-induced changes in the solubility of these hydrophobic substances. A stock solution of the HPCD complex of 1-PB was prepared on a vortex mixer by mixing 1 volume of a 10 mM acetone solution of 1-PB with 2 volumes of a 30 mg/mL solution of HPCD in 0.1 M Na-Hepes buffer (pH 7.4). A 2.5 mM stock solution of the HPCD complex of testosterone in the buffer described above was prepared using commercially available HPCD-encapsulated testosterone. Control studies presented in the Supporting Information showed that replacement of the stock solutions of 1-PB and testosterone in acetone with their water-soluble

complexes with HPCD has virtually no effect on the parameters of the interactions of these substrates with CYP3A4 (Figure S4). Therefore, although an increase in hydrostatic pressure results in gradual dissociation of the HPCD complexes (Figure S5), this process is not expected to have any appreciable effect on the barotropic behavior of the enzyme.

Data Processing. To interpret the experiments in terms of pressure-induced changes in the concentration of P450 and P420, we used principal component analysis (PCA) as described previously (*26*, *37*). This approach allowed us to increase significantly the signal-to-noise ratio and to remove the spectral perturbations due to the changes in the turbidity of the system during the experiments. To interpret the pressure-induced transitions in terms of changes in the concentration of P450 species, we used a least-squares fitting of the spectra of principal components to the set of the spectral standards of pure high-spin P450, low-spin P450, and P420 species of the heme protein (*11*, *38*). Prior to the analysis, all spectra were corrected for the compression of the solvent, as described previously (*25*).

Our interpretation of the pressure-induced changes is based on the equation for the pressure dependence of the equilibrium constant (*39*; eq 1)

$$\partial(\ln K_{eq})/\partial p = -(\Delta V^\circ)/RT \quad (1)$$

or [in integral form (page 212 of ref *40*, eq 9)]

$$K_{eq} = K_{eq}^\circ e^{-P\Delta V^\circ/RT} = e^{(P-P)\Delta V^\circ/RT} \quad (2)$$

where K_{eq} is the equilibrium constant of the reaction at pressure P, $P_{1/2}$ is the pressure at which $K_{eq} = 1$ ("half-pressure" of the conversion), ΔV° is the standard molar reaction volume, and K_{eq}° is the equilibrium constant extrapolated to zero pressure ($K_{eq}^\circ = e^{P_{1/2}\Delta V^\circ/RT}$). For the A $\rightleftharpoons$ B equilibrium and when $K_{eq}^\circ = [B]/[A]$, eq 2 produces the following relationship:

$$[A] = \frac{C_0}{1 + K_{eq}^\circ e^{-P\Delta V^\circ/RT}} = \frac{C_0}{1 + e^{(P_{1/2}-P)\Delta V^\circ/RT}} \quad (3)$$

where $C_0 = [A] + [B]$. Curve fitting was performed using our SPECTRALAB software package (*26*).

RESULTS

Pressure-Induced Transitions in CYP3A4 Incorporated into Nanodiscs. As shown in our previous publication, application of elevated hydrostatic pressure to oligomeric CYP3A4 in solution results in a reversible high to low shift of the spin equilibrium, which is followed by a P450 → P420 transition. This apparent inactivation process involves no more than 72 ± 6% of the heme protein and is slowly reversible upon decompression (*11*). In addition to this rapid P450 → P420 transition, there was a slower irreversible inactivation process, which takes place upon prolonged incubation of the protein at pressures of >1500 bar. This apparent conformational heterogeneity of the protein disappeared upon monomerization of CYP3A4 in the presence of detergent (*11*). To rule out the possible involvement of a direct interaction of detergent with CYP3A4 in the effect described above, we have now studied the pressure-induced transitions of CYP3A4 monomerized by incorporation into lipoprotein Nanodiscs (CYP3A4ND).

Control experiments described in the Supporting Information demonstrated that the tryptophan fluorescence of CYP3A4-containing Nanodiscs exhibits a gradual decrease at increased hydrostatic pressures. This process was completely reversible upon decompression from 4.8 kbar (Figure S2). Therefore, the pressure-induced changes in the Nanodiscs are reversible, and the elevated pressure does not cause a destruction of their assembly. We also studied the fluorescence of DCVJ as a probe of the microviscosity of the lipid phase (*41*) to monitor possible pressure-induced changes that might influence CYP3A4 transitions. The results of these control experiments described in the Supporting Information demonstrated that the pressure-induced increase in the viscosity of the lipid phase is completely reversible and is characterized by a ΔV° of −21 mL/mol and a $P_{1/2}$ of 4.3 kbar (Figure S3). The small changes in the lipid viscosity below 2.5 kbar, where most of the pressure-induced changes in the spin equilibrium and substrate binding in CYP3A4 are observed, do not seem to affect the barotropic behavior of the enzyme.

The effect of hydrostatic pressure on the absorbance spectra of CYP3A4ND in the presence of a saturating concentration of BCT is illustrated in Figure 1a along with the changes in the concentrations of the high-spin, low-spin, and P420 states of CYP3A4ND (inset). Although the observed transitions are qualitatively similar to those in CYP3A4 oligomers, the spin shift and P450 → P420 transitions are considerably better resolved in CYP3A4ND. The pressure dependencies of the P420 content in CYP3A4ND in the presence of increasing concentrations of BCT are shown in Figure 1b. In contrast to CYP3A4 oligomers, where only approximately two-thirds of the total heme protein was susceptible to this process (*11*), the amplitude of the P450 → P420 transition in CYP3A4ND comprises 93 ± 3%, regardless of the substrate concentration. It should be noted that in CYP3A4ND we observed no slow, irreversible P450 → P420 conversion of the kind noted with CYP3A4 oligomers (*11*). The partitioning between P450 and P420 states of CYP3A4ND reaches its steady state in less than 1 min after a pressure increase and reverses completely within 5−10 min upon decompression (data not shown). These results are consistent with our initial conclusion that the heterogeneity of P450 in solution in sensitivity to a pressure-induced P450 → P420 transition is due to the oligomerization of the enzyme.

CYP3A4ND also differs from the oligomeric enzyme by an increased value of ΔV°_{P420}. In CYP3A4ND, the volume change in the P450 → P420 transition was as large as −86.9 ± 6.4 mL/mol and revealed no dependence on substrate concentration, while the value of $P_{1/2}$ exhibited a distinct increase upon substrate saturation (Figure 1). This finding is also in contrast to CYP3A4 oligomers in solution, where ΔV°_{P420} changes from −25 ± 4 to −41 ± 3 mL/mol (*11*), and the changes in $P_{1/2}$ were marginal. Therefore, monomerization by incorporation into Nanodiscs stabilizes the enzyme with regard to pressure-induced inactivation by increasing the reaction volume change of the P450 → P420 transition. Formation of the complex of CYP3A4ND with BCT results in a further decrease in the susceptibility of the

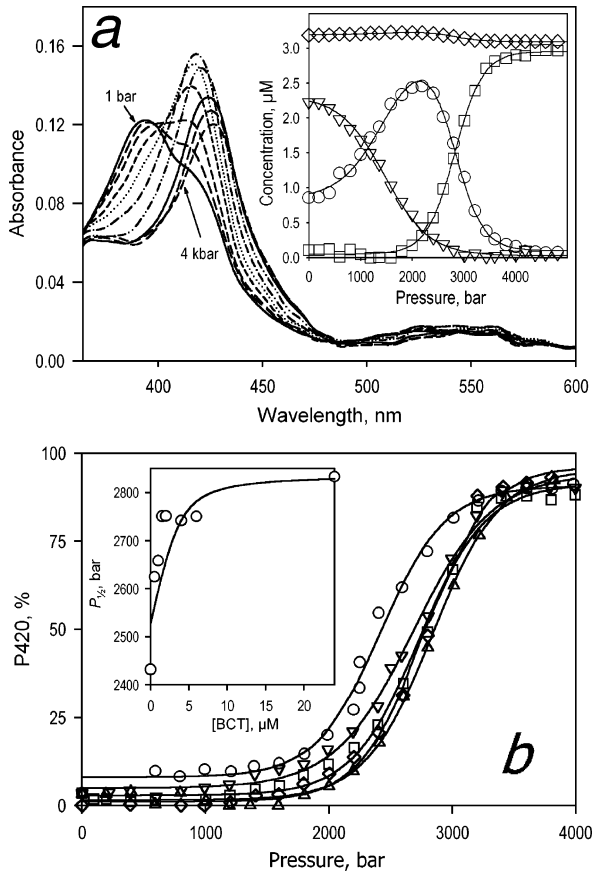

FIGURE 1: Pressure-induced transitions in CYP3A4 in Nanodiscs in the presence of BCT. (a) A series of spectra in the presence of 24 μM BCT recorded at 1 bar (solid line), 800 bar (long dash line), 1200 bar (medium dash line), 1600 bar (short dash line), 2000 bar (dotted line), 2400 bar (dashed−dotted line), 2800 bar (dashed−dotted−dotted line), 3200 bar (solid line), 3600 bar (long dashed line), and 4000 bar (medium dashed line). Conditions: 3.2 μM CYP3A4ND in 0.1 M Na-Hepes buffer (pH 7.4), 1 mM DTT, 1 mM EDTA, 25 °C, optical path length of 0.5 mm. The inset shows the corresponding changes in the concentration of the high-spin (▽), low-spin (○), and P420 (□) states of CYP3A4 and the total hemoprotein concentration (◇). Panel b illustrates the course of the pressure-induced P450 → P420 transition with no substrate added (○) and with 0.5 (△), 1.5 (□), 2 (◇), and 24 μM BCT (▽). Solid lines represent the results of fitting of these curves to eq 3. The inset of panel b shows the dependence of $P_{1/2}$ found by this fitting on BCT concentration. The corresponding $\Delta V°$ values were in the range of 84−94 mL/mol and showed no systematic trend with BCT concentration.

enzyme to pressure-induced inactivation by increasing the $P_{1/2}$ of this process.

Analysis of the Effect of Hydrostatic Pressure on the Spin Equilibrium of CYP3A4 in the Presence of Increasing Concentrations of BCT. While our previous publication and the data given above clarify the pressure-induced P450 → P420 transition in CYP3A4, the pressure-induced spin shift and the effect of pressure on the affinity of the enzyme for substrates remain to be characterized. To resolve the barotropic parameters of the spin transitions of the substrate-free and BCT-bound CYP3A4 from those of the dissociation of the BCT complex with the enzyme, we studied the pressure-induced spin transitions of CYP3A4 in oligomers in solution and CYP3A4ND at a series of BCT concentrations ranging from 0 to 24 μM. In agreement with earlier results (*11*, *42*), our ambient-pressure titration experiments showed no homotropic cooperativity and a high amplitude

Table 1: Parameters of Interactions of CYP3A4 with Substrates at Ambient Pressure[a]

system	substrate	K_D or S_{50}	n	ΔF_h(max) (%)[b]
3A4 in solution	BCT	0.31 ± 0.1	N/A[c]	33 ± 6
	testosterone	88 ± 16	1.21 ± 0.04	36 ± 8
	1-PB	10.6 ± 0.7	1.55 ± 0.2	42 ± 8
3A4ND	BCT	0.39 ± 0.2	N/A[c]	51 ± 18
	testosterone	100 ± 8	1.62 ± 0.2	46 ± 3

[a] The values represent the averages of the results of three to six individual absorbance titration experiments at ambient pressure. In the titrations with testosterone and 1-PB, stock solutions of the complexes of the substrates with HPCD in 0.1 M Na-Hepes buffer (pH 7.4) were used (see Materials and Methods). [b] Maximal amplitude of substrate-induced spin shift. [c] Not applicable.

of the substrate-induced spin shift in the interactions of this high-affinity substrate with CYP3A4ND (Table 1). As seen from Figure 2a, addition of BCT increases considerably the amplitude of the pressure-induced spin shift. The same results are presented in Figure 2b as dependencies of the high-spin content of CYP3A4ND on BCT concentration (e.g., binding isoterms) at variable pressure.

The curves shown in Figure 2b may be adequately fitted by the equation for the equilibrium of binary association (in ref *43*, eq II-53, on page 73) modified to account for a non-zero offset (A_0) and an adjustable coefficient of proportionality between the concentration of the complex and the observed signal (A_{max}) to yield the values of K_D at respective pressures:

$$A([S]_0) = A_0 + A_{max}([ES]/[E]_0) = A_0 + A_{max} \times \left\{ \frac{[E]_0 + [S]_0 + K_D - [([E]_0 + [S]_0 + K_D)^2 - 4[E]_0[S]_0]^{1/2}}{2[E]_0} \right\} \quad (4)$$

where $A([S]_0)$ represents the amplitude of a signal evidencing the substrate binding (high-spin fraction of the enzyme in our case) at substrate concentration $[S]_0$.

The equilibrium constants of the spin equilibrium for the substrate-free ($K_{h,free}$) and BCT-bound enzyme ($K_{h,BCT}$) may be found from the high-spin content at no substrate added and at saturating BCT given by the A_0 and A_{max} values. The dependencies of the logarithms of $K_{h,free}$, $K_{h,BCT}$, and K_D on pressure shown in panels a and b of Figure 3 exhibit a clear break around 800−1000 bar, which is unexpected. Fundamental eqs 1 and 2 suggest the pressure dependency of the logarithm of an equilibrium constant to be linear, with a slope determined by the standard reaction volume change in the pressure-induced transition. Observation of a break in these plots suggests that, in addition to the substrate binding and spin equilibria per se, CYP3A4ND exhibits an additional pressure-dependent transition affecting the $\Delta V°$ values of the processes described above. In other words, the enzyme appears to be subjected to a pressure-dependent equilibrium between two distinct states having different barotropic parameters of the spin transitions and BCT binding. We designate these two putative conformational states of the protein as R (for relaxed) and P (for pressure-promoted) states and refer to the transition between them as the R → P transition.

To determine the barotropic parameters of the R → P transition, we plotted the first derivatives of the logarithms

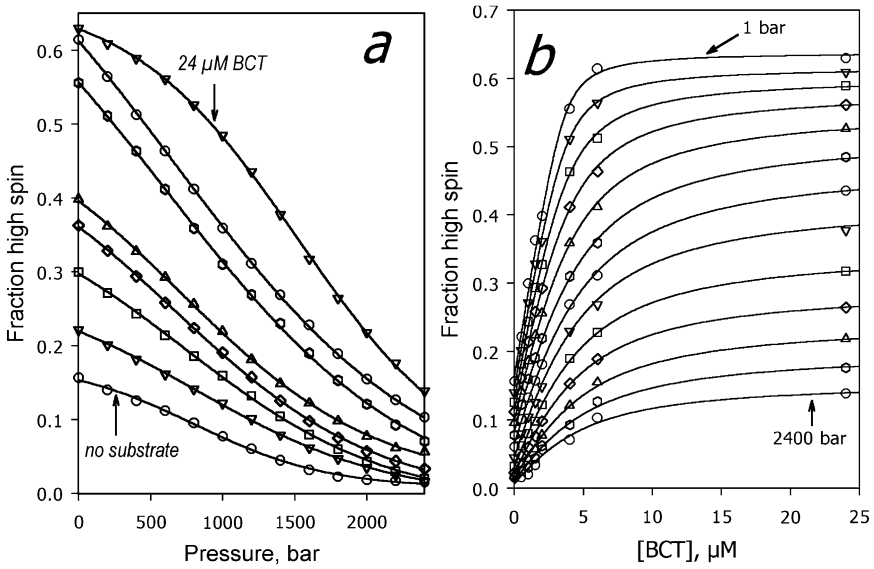

FIGURE 2: Effect of hydrostatic pressure on the spin state of CYP3A4 in Nanodiscs at increasing concentrations of bromocriptine. Panel a shows the dependencies of the high-spin content in CYP3A4ND on pressure at no substrate added (○) and with 0.5 (▽), 1 (□), 1.5 (◇), 2 (△), 4 (⬡), 6 (○), and 24 μM BCT (▽). Solid lines represent the results of fitting of these curves to eq 3. Panel b shows the same data set as the dependencies of the high-spin content on substrate concentration at a series of hydrostatic pressures increasing from 1 to 2400 bar in 200 bar increments. Solid lines show the results of fitting of the titration curves to eq 4. Conditions as described in the legend of Figure 1.

of $K_{h,free}$, $K_{h,BCT}$, and K_D versus pressure. As shown in Figure 3 (right panels), these plots are represented by sigmoidal curves obeying the equation for pressure dependence of the concentration of a compound subjected to an equilibrium transition (eq 3). The fitting of these curves yields the values of $\Delta V°$ of −69 mL/mol for both constants of spin transitions ($K_{h,free}$ and $K_{h,BCT}$) and −98 mL/mol for the constant of dissociation of the substrate complex (K_D).

Similar behavior was also observed in the oligomers of CYP3A4 in solution, where the parameters of the interactions of the enzyme with BCT at ambient pressure were close to those observed in CYP3A4ND (Table 1). The plots of the high-spin content in CYP3A4 versus pressure at different concentrations of BCT are shown in Figure 4a. The corresponding dependencies of the high-spin fraction on BCT concentration at different pressures obey the equation for the equilibrium of binary association (Figure 4b), and the plots of the logarithms of $K_{H,free}$, $K_{H,BCT}$, and K_D on pressure exhibit distinct breaks in the range of 1000−1500 bar (Figure 5a,b). The break in the plot for ln(K_D) is especially illustrative, as it reflects the change in the sign of $\Delta V°$, so that an increase in hydrostatic pressure in the low-pressure range results in dissociation of the complex, whereas BCT binding is promoted at pressures of >1500 bar. Similar to the observations with CYP3A4ND, the plots of the derivatives of the logarithms of the equilibrium constants versus pressure reveal a pressure-induced transition in CYP3A4 in solution, which changes the values of $\Delta V°_{H,free}$, $\Delta V°_{H,BCT}$, and $\Delta V°_{diss}$ (Figure 5, right panels). The values of $\Delta V°$ of this transition determined from the plots for $K_{H,free}$, $K_{H,BCT}$, and K_D are as large as −50 to −90 mL/mol (Table 2). The remarkable similarity of these results to those reported above for CYP3A4ND suggests that the incorporation of CYP3A4 into Nanodiscs and possible pressure-induced rearrangements in the scaffold protein and/or lipid bilayer have no significant effect on the observed barotropic behavior of the enzyme in Nanodiscs.

Analysis of the Effect of Hydrostatic Pressure on the Spin Equilibrium of CYP3A4 in Nanodiscs and in Solution in the Presence of Substrates Demonstrating Homotropic Cooperativity. The results presented above reveal a pressure-dependent equilibrium between two states of the enzyme that affects the BCT-induced spin transitions in both CYP3A4ND and CYP3A4 in solution. To probe the possible involvement of this apparent conformational transition in the mechanisms of cooperativity of CYP3A4, we studied the effect of hydrostatic pressure on the spin state of CYP3A4 in the presence of various concentrations of testosterone and 1-PB, type I substrates with which homotropic cooperativity is observed. The HPCD complexes of the substrates were used to approach saturating concentrations and minimize the effect of pressure-induced changes in solubility. The parameters of the interactions of CYP3A4 with these substrate obtained from the ambient-pressure titration experiments are given in Table 1. It should be noted, however, that due to a profound decrease in the affinity for 1-PB observed upon incorporation of CYP3A4 into the Nanodiscs (data not shown), the studies of the interactions of CYP3A4ND with this substrate were precluded by its low solubility and high extinction coefficient in the Soret region. Therefore, the studies with the enzyme incorporated into the Nanodiscs were limited to the case of testosterone only.

The pressure-induced changes in CYP3A4ND in the presence of 280 μM testosterone are illustrated in Figure 6a. Comparison of this figure with the transitions observed in the presence of BCT in CYP3A4 in Nanodiscs (Figure 1) and in solution (ref *11* and Figure 3) reveals a critical difference. Namely, the pressure dependence of the spin state in the presence of testosterone has a considerably lower amplitude than in the complex of the enzyme with BCT. Even at a pressure as high as 4 kbar, there is a significant high-spin CYP3A4 content in the presence of testosterone. In contrast, both in solution and in Nanodiscs, there is no high-spin heme protein above 3 kbar in the absence of

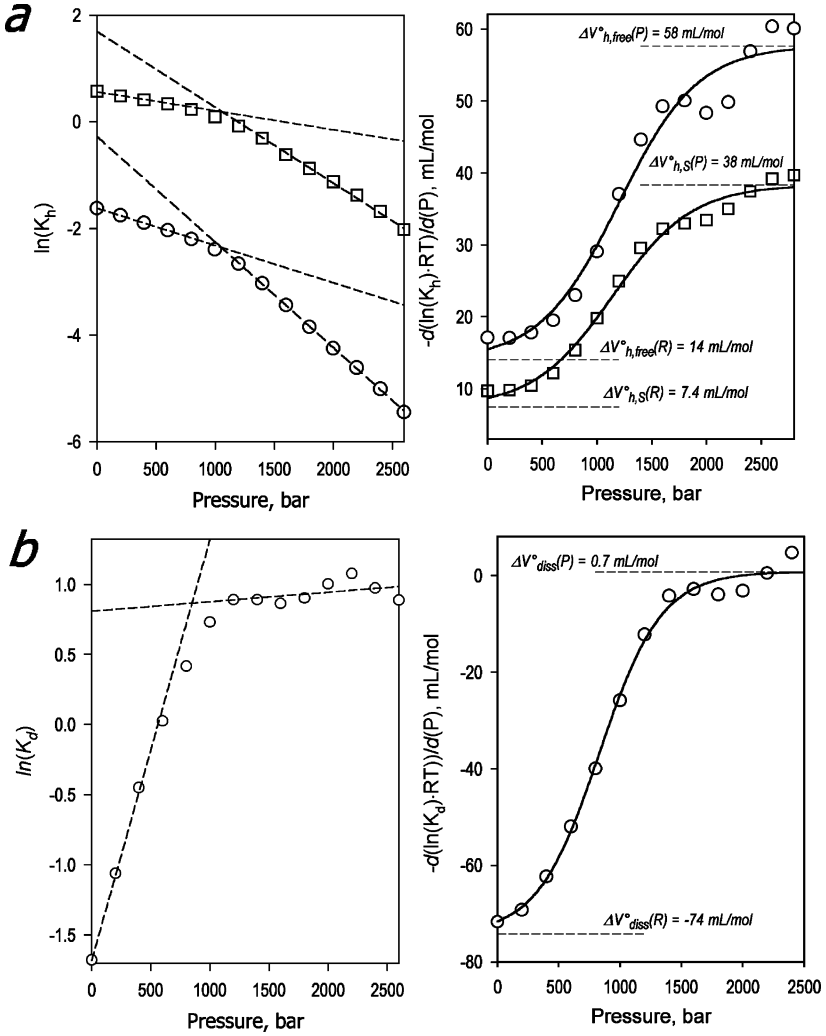

FIGURE 3: Effect of hydrostatic pressure on the parameters of spin equilibrium and BCT binding in CYP3A4ND. The top panels (a) illustrate the effect of hydrostatic pressure on the constant of spin equilibrium of the substrate-free (○) and BCT-bound enzyme (□). The bottom panels (b) exemplify the pressure dependence of the dissociation constant of the BCT complex of the enzyme. The left panels show the pressure dependencies of the logarithms of the respective constants, whereas the right panels represent the first derivatives of the above dependencies approximated by a fifth-order polynomial. Dashed lines shown in the left panels show a linear approximation of the initial and final parts of the curves. Solid lines shown in the right panels represent the results of fitting of the respective data sets to eq 3 with the parameters listed in Table 2. The low- and high-pressure limits of the respective fitting curves shown in the right panels give the ΔV° values that characterize the putative R and P conformational states of the enzyme, respectively.

substrate or presence of BCT. Similar behavior was also observed for CYP3A4 in solution in the presence of either testosterone (Figure 6b) or 1-PB (Figure 6c). To rule out the possible involvement of interactions of the substrate with HPCD, we also performed a series of experiments with CYP3A4 in solution in the presence of 1-PB added as a 15 mM stock solution in acetone with no HPCD present. The behavior of CYP3A4 revealed in these experiments was similar to that shown in Figure 6c for the complex of 1-PB with HPCD (data not shown).

The difference in the barotropic behavior of CYP3A4 with 1-PB and testosterone as opposed to BCT becomes especially evident from the analysis of the pressure-induced changes in the spin state of CYP3A4 observed at various substrate concentrations. As one can see from Figure 7a (left panel), although displacing the spin equilibrium toward the high-spin state, testosterone does not increase the amplitude of the pressure-induced spin shift to the same extent. Consequently, in contrast to other cytochrome P450 species where the amplitude of the substrate-induced spin shift at elevated pressures approaches zero (*26*, *31*, *39*), the substrate-induced spin shift in the interactions of CYP3A4ND with testosterone remains considerable even at pressures above 2000 bar, where no further decrease in the high-spin content is observed (Figure 7a, right panel). A similar phenomenon was observed with CYP3A4 in solution with both testosterone (Figure 7b) and 1-PB (Figure 7c). This unusual behavior of CYP3A4 with substrates exhibiting homotropic cooperativity is especially evident in the case of the interactions of CYP3A4 in solution with 1-PB (Figure 7c, left panel). Importantly, similar barotropic behavior was also observed in preliminary studies of the interactions of CYP3A4 in solution with α-naphthoflavone, another substrate exhibiting homotropic cooperativity (data not shown).

Analysis of the pressure dependence of the constant of spin equilibrium in the complexes of CYP3A4ND and CYP3A4 in solution is illustrated in Figure 8. In common with observations of the interactions of CYP3A4 with BCT, the nonlinear pressure dependencies of $\ln(K_h)$ in the complexes of CYP3A4 with testosterone and 1-PB (Figure 8a) suggest a pressure-dependent equilibrium between two states of the enzyme characterized by different values of ΔV°_{spin}.

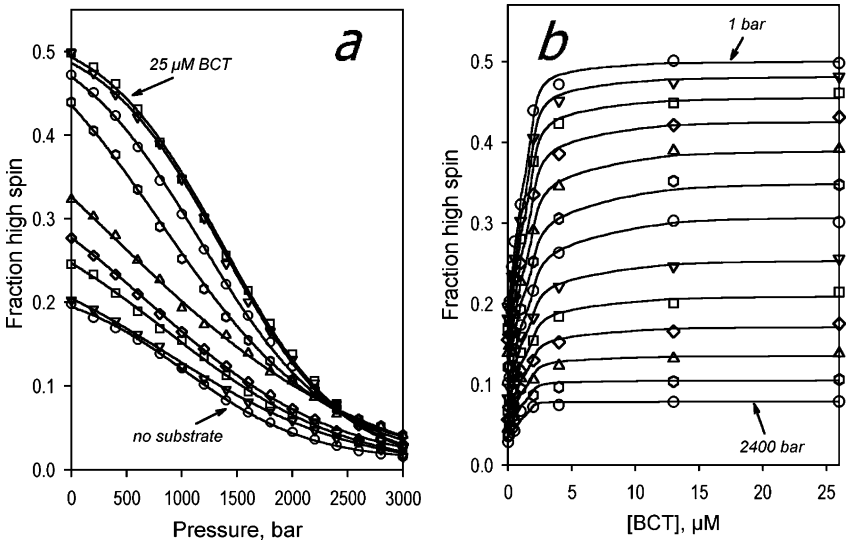

FIGURE 4: Effect of hydrostatic pressure on the spin state of CYP3A4 in solution at increasing concentrations of BCT. Panel a shows the dependencies of the high-spin content on pressure with no substrate added (○) and with 0.1 (▽), 0.35 (□), 0.5 (◇), 1.0 (△), 2.0 (⬡), 4.0 (○), 13 (▽), and 24 μM BCT (□). Solid lines represent the results of fitting of these curves to eq 3. Panel b shows the same data set as the dependencies of the high-spin content on the substrate concentration at a series of hydrostatic pressures increasing from 1 to 2400 bar in 200 bar increments. Solid lines show the results of fitting of the titration curves to eq 4. Conditions as described in the legend of Figure 1, except for the concentration of CYP3A4, which was equal to 2 μM.

However, in contrast to the substrate-free enzyme and the complexes of CYP3A4 with BCT, where this putative R → P transition resulted in an *increase* in the value of $\Delta V°_{spin}$, the complexes of both CYP3A4 oligomers and CYP3A4ND with allosteric substrates reveal an important *decrease* in $\Delta V°_{spin}$ with the transition to the pressure-promoted conformation. The molar volume change in the spin transition approaches zero upon the conversion of the complexes of CYP3A4 with testosterone and 1-PB into the pressure-promoted state (Table 2).

The analysis of the pressure dependence of substrate binding isotherms shown in the right panels of parts b and c of Figure 8 suggests an important increase in the cooperativity of the interactions at elevated pressures, where the values of the Hill coefficient for the interactions of CYP3A4 in solution with testosterone and 1-PB approach 3.3 and 1.9, respectively (Figure 9). In both cases, this increase in cooperativity was associated with changes in S_{50} values analogous to those shown in Figure 5b for the K_D of the complex of CYP3A4 with BCT (data not shown). An initial increase in the S_{50} values with an increase in pressure is followed by a sharp decrease at pressures of >1200 bar. This behavior is also consistent with a pressure-induced conformational transition in the enzyme that changes the sign of the volume changes observed upon substrate dissociation (Table 2). In contrast, no considerable pressure-induced changes in the values of S_{50} and the Hill coefficient for the interactions with testosterone were observed in CYP3A4ND (data not shown). These results suggest that homotropic cooperativity in CYP3A4 represents a true case of allostery that involves transitions between several conformational states of the enzyme characterized by different values of $\Delta V°_{spin}$ and $\Delta V°_{diss}$. Interactions of the enzyme with the allosteric substrates appear to induce a conformational transition that decreases the water accessibility and/or the degree of hydration of the active site so that the flux of water into the heme pocket is impeded and the high-spin state of the heme iron is stabilized.

DISCUSSION

Our pressure-perturbation experiments on CYP3A4−substrate interactions using enzyme in solution and in Nanodiscs have yielded three pivotal findings that have broad implications for an understanding of cytochrome P450 function and cooperativity. First, with both kinds of CYP3A4 preparations, there are some striking differences between this allosteric enzyme and the other cytochrome P450 species studied previously in several laboratories. Second, the barotropic behavior of CYP3A4 differs dramatically in the presence of the allosteric substrates testosterone and 1-PB as opposed to the non-allosteric substrate BCT. Third, differences between the behavior of oligomeric CYP3A4 in solution compared with the monomeric enzyme in Nanodiscs confirm and extend our previous findings on the existence of stable, functionally distinct conformers in the oligomers. Overall, pressure-perturbation spectroscopy promises to be an invaluable complement to other approaches our laboratory has introduced recently for analysis of mechanisms of CYP3A4 cooperativity (*1*, *2*, *38*).

In contrast to CYP2B4, P450cam, and P450 BMP, which exhibit no apparent changes in $\Delta V°_{H,free}$, $\Delta V°_{H,S}$, and $\Delta V°_{diss}$ with pressure, CYP3A4 revealed a pressure-induced transition that changes the values of $\Delta V°$ of the substrate dissociation and spin transitions. This important difference between CYP3A4 and other P450 heme proteins studied to date is especially evident upon comparison of Figures 3, 5, and 8 with Figure 10, which shows similar plots for the heme domain of cytochrome P450 BM3 (BMP) based on our earlier results (*31*).

Four states of P450 are routinely considered in the analysis of substrate- and pressure-induced spin transitions (*26*, *31*, *39*), namely, the low- and high-spin states of both the substrate-free and substrate-bound enzyme. Our studies reveal an additional pressure-sensitive equilibrium between two distinct conformational states of CYP3A4, designated here as R (for relaxed) and P (for pressure-promoted) states. The

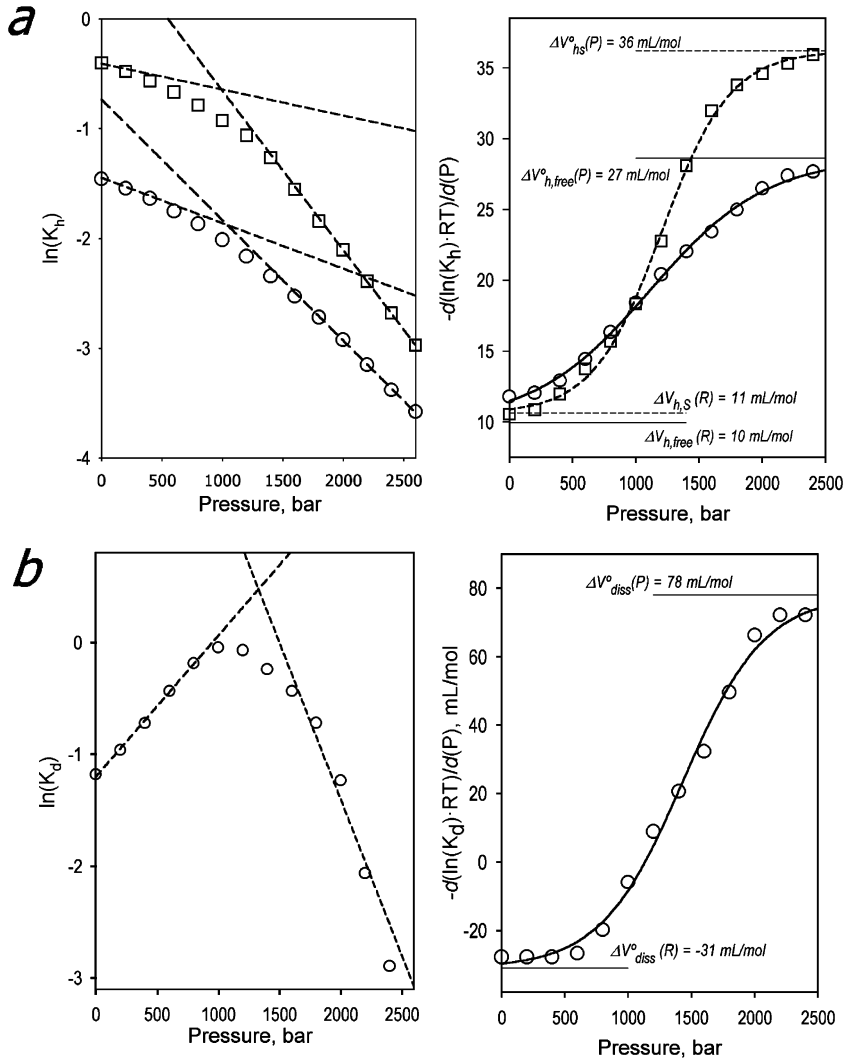

FIGURE 5: Effect of hydrostatic pressure on the parameters of spin transitions and dissociation of the complex of CYP3A4 in solution with BCT. The designation of the panels and the keys are similar to those specified for Figure 3.

Table 2: Parameters of Pressure-Dependent Equilibria in CYP3A4

						parameters of R → P transition[a]			
		$\Delta V°_{spin}$ (mL/mol)		$\Delta V°_{diss}$ (mL/mol)		based on pressure dependence of K_h		based on pressure dependence of K_d (S_{50})	
substrate	system	R state	P state	R state	P state	$\Delta V°_{R\rightarrow P}$ (mL/mol)	$K_{R\rightarrow P}$ at 1 bar	$\Delta V°_{R\rightarrow P}$ (mL/mol)	$K_{R\rightarrow P}$ at 1 bar
none	3A4ND	14	58	N/A[b]	N/A[b]	−69	0.04	N/A[b]	N/A[b]
	3A4 in solution	10	27	N/A[b]	N/A[b]	−54	0.09	N/A[b]	N/A[b]
BCT	3A4ND	7.4	38	−74	0.7	−69	0.04	−98	0.04
	3A4 in solution	11	36	−31	78	−91	0.01	−77	0.01
testosterone	3A4ND	34	−5	0	0	−52	0.3	N/A[b]	N/A[b]
	3A4 in solution	32	0	−15	11	−42	0.13	−45	0.16
1-PB	3A4 in solution	9.1	−1	−6.7	8.5	−58	0.07	−52	0.07

[a] Barotropic parameters of the R → P transition obtained from the fitting of the first-derivative plots for $\ln(K_h)$, $\ln(K_d)$, or $\ln(S_{50})$ to eq 3. Values of the constant of the R ↔ P equilibrium were derived from the corresponding $P_{1/2}$ and $\Delta V°$ values according to eq 2. [b] Not applicable.

pressure-induced transition between these states causes a nonlinearity of the plots of the logarithms of the apparent values of $K_{H,free}$, $K_{H,S}$, and K_D versus pressure. It is important to note that the nonlinearity of the plots is observed in oligomeric CYP3A4 in solution (Figures 5 and 8b,c) as well as monomeric CYP3A4ND (Figures 3 and 8a), suggesting that this apparent pressure-sensitive conformational equilibrium constitutes an inherent feature of the CYP3A4 monomer.

The slope of the plots of the logarithms of the constants of equilibrium versus pressure is therefore determined by the partitioning between the R and P states at each given pressure so that the dependencies of $-d[\ln(K_{eq}) \times RT]/d(P)$ on pressure reflect the changes in the fraction of the pressure-promoted P state. Fitting of these derivative plots (Figures 3, 5, and 8, right panels) to eq 3 allows us to determine the barotropic parameters of the transition between these two conformations of the enzyme (Table 2). As CYP3A4ND and

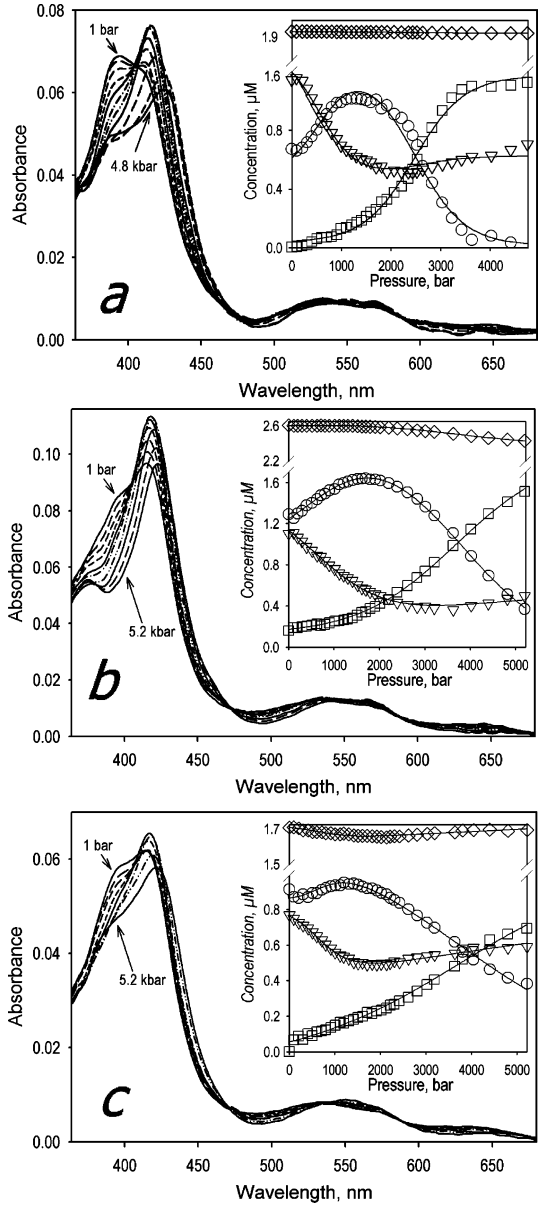

FIGURE 6: Pressure-induced transitions in CYP3A4 in the presence of testosterone and 1-PB. (a) A series of spectra of CYP3A4ND in the presence of 280 μM testosterone obtained at 1 bar (solid line), 300 bar (long dashed line), 400 bar (medium dashed line), 600 bar (short dashed line), 800 bar (solid line), 1200 bar (dashed−dotted line), 1600 bar (dashed−dotted−dotted line), 2000 bar (solid line), 2800 bar (long dashed line), 3600 bar (medium dashed line), and 4800 bar (solid line). (b) A series of spectra of CYP3A4 oligomers in solution in the presence of 420 μM testosterone obtained at 1 bar (solid line), 200 bar (long dashed line), 400 bar (medium dashed line), 800 bar (short dashed line), 1200 bar (solid line), 2000 bar (dashed−dotted line), 3600 bar (dashed−dotted−dotted line), and 5200 bar (solid line). (c) A series of spectra of CYP3A4 oligomers in solution in the presence of 16 μM 1-PB obtained at 1 bar (solid line), 400 bar (long dashed line), 800 bar (medium dashed line), 1200 bar (short dashed line), 1600 bar (solid line), 2000 bar (dashed−dotted line), 2800 bar (dashed−dotted−dotted line), 3600 bar (solid line), 4400 bar (long dashed line), and 5200 bar (solid line). The insets show the corresponding changes in the concentration of the high-spin (▽), low-spin (○), and P420 (□) states of CYP3A4 and the total hemoprotein concentration (◇). Conditions as described in the legend of Figure 1, except for the concentration of CYP3A4, which was equal to 1.9, 2.5, and 1.7 μM for panels a−c, respectively.

the enzyme in solution both revealed a considerable negative volume change (from −45 to −98 mL/mol) in the R → P transition in both the substrate-free enzyme and the complexes with BCT, testosterone, and 1-PB, this transition is likely to involve an important increase in the extent of protein hydration.

The most striking observation in this study is that the enzyme saturated with testosterone or 1-PB becomes refractory to pressure-induced displacement of spin and substrate binding equilibria upon the transition to the P state (at pressures of >1600 bar). Insight into the mechanistic basis of this unusual behavior becomes possible upon analysis of the plots of the derivatives of $\ln(K_h)$ and $\ln(S_{50})$ versus pressure. The limits that these plots approach at infinitely increasing or decreasing pressure provide us with estimates of the corresponding ΔV° values for the P and R states, respectively. Analysis of these values (Table 2) reveals an important difference between the substrate-free or BCT-bound enzyme and the complexes of CYP3A4 with testosterone or 1-PB. In contrast to the substrate-free or BCT-bound enzyme, where the R → P transition results in a considerable increase in the positive value of ΔV°_{spin} (Table 2), the R → P transition of the complexes of the enzyme with allosteric substrates causes a decrease in ΔV°_{spin} to zero or even negative values, as in the complex of CYP3A4ND with testosterone (Table 2). This difference in the mechanisms of interactions is also revealed in the values of ΔV°_{diss}. Whereas the dissociation of the BCT complexes of the R state of either CYP3A4 in solution or CYP3A4ND is associated with an important negative volume change (−74 or −31 mL/mol, respectively), the value of ΔV°_{diss} of the complexes of the R state of CYP3A4 with allosteric substrates is as low as −15 or −7 mL/mol (in the complexes of CYP3A4 in solution with testosterone or 1-PB, respectively) or even equal to 0, as in the case of the complex of CYP3A4ND with testosterone. Furthermore, in the case of CYP3A4 in solution, the R → P transition results in a change in the sign of ΔV°_{diss} of the complexes with testosterone and 1-PB (Table 2). Due to such non-negative values of ΔV°_{diss} in the pressure-promoted state, elevated hydrostatic pressure is incapable of causing complete dissociation of the complexes of CYP3A4ND or CYP3A4 oligomers with allosteric substrates. This observation coupled with the above finding that the values of ΔV°_{spin} of these complexes approach zero or even change sign upon the transition to the P state (Table 2) explains why elevated pressure cannot displace the spin equilibrium in these complexes completely to the low-spin state.

The observation that elevated hydrostatic pressure induces an important increase in the cooperativity of CYP3A4 in solution with either testosterone or 1-PB (Figure 9) suggests a tight connection between the R ↔ P conformational equilibrium and the mechanisms of cooperativity. Interestingly, the dependencies of the Hill coefficient on pressure fit adequately to eq 3 for the pressure dependency of equilibrium (Figure 9, solid lines), with the ΔV° values of −56 and −69 mL/mol for the cases of testosterone and 1-PB, respectively, which are consistent with the values for the R → P transition derived from the analysis of the derivative plots (Table 2). Involvement of the R → P transition in the mechanisms of cooperativity is also revealed in a displacement of the conformational equilibrium toward the P state by testosterone observed in both CYP3A4 in solution and CYP3A4ND (Table 2).

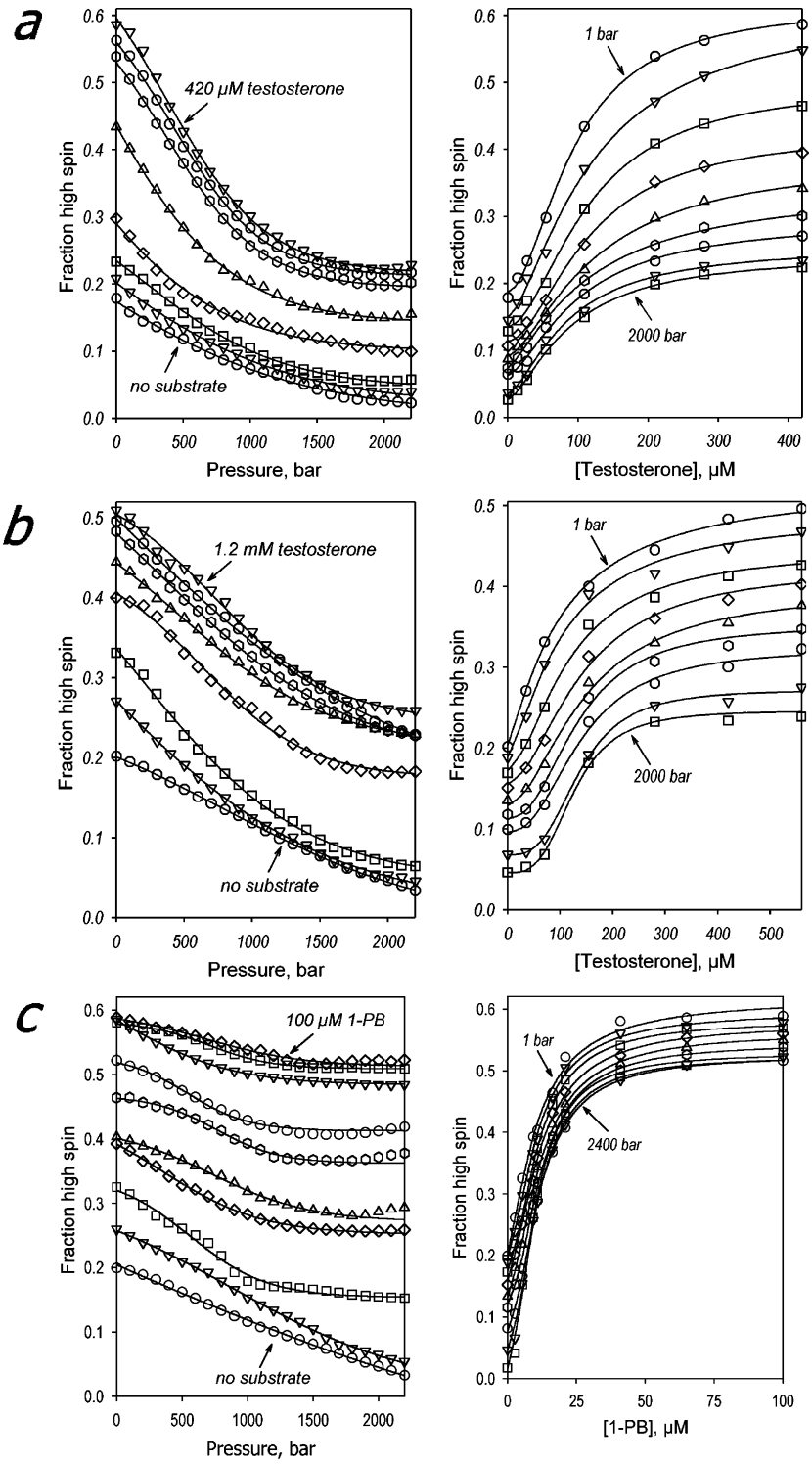

FIGURE 7: Effect of hydrostatic pressure on the spin state of CYP3A4 at increasing concentrations of allosteric substrates. Panel a illustrates the behavior of CYP3A4ND with testosterone (TST), while panels b and c represent the transitions observed with CYP3A4 in solution in the presence of testosterone and 1-PB, respectively. Left panels show the dependencies of the high-spin content on pressure at various substrate concentrations. Solid lines represent the results of fitting of these curves to eq 3. The curves shown in panel a correspond to no substrate added and to 14, 28, 56, 112, 210, 280, and 420 μM testosterone added. The data shown in panel b represent the dependencies obtained with no substrate added and with 35, 70, 154, 280, 420, 560, and 1225 μM testosterone added. The data represented in panel c correspond to no substrate added and 2.7, 5.4, 9.3, 11, 16, 21, 41, and 100 μM 1-PB added. Right panels show the same data set as the dependencies of the high-spin content on the substrate concentration at a series of hydrostatic pressures increasing from 1 to 1600 bar in 200 bar increments and at 2000 bar. The curves obtained at 800, 1200, and 1400 bar are omitted from panel c for clarity. Solid lines show the results of fitting of the titration curves to the Hill equation. Conditions as described in the legend of Figure 6.

Accordingly, our results suggest that the mechanisms of cooperativity in CYP3A4 involve a complex system of transitions in an ensemble of conformational states differing in the degree of hydration and water accessibility of the heme pocket. Although we are far from a detailed understanding of the conformational dynamics of the enzyme involved in the allosteric mechanisms, our results led us to the following basic assertions. In the absence of substrate, the enzyme is

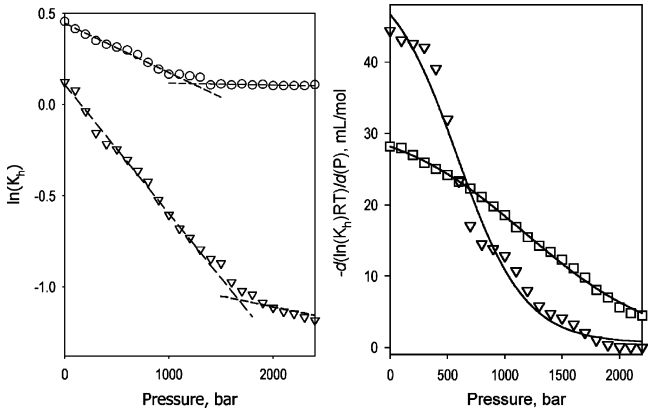

FIGURE 8: Effect of hydrostatic pressure on the constant of spin equilibrium for the complexes of CYP3A4ND with testosterone (▽) and CYP3A4 in solution with either testosterone (□) or 1-PB (○). The left panel illustrates the pressure dependencies of the logarithms of $K_{h,S}$, whereas the right panels show the first derivatives of the above dependencies approximated by a fifth-order polynomial. Dashed lines shown in the left panel represent a linear approximation of the initial and final parts of the curves. Solid lines shown in the right panels show the results of fitting of the respective data sets to eq 3 with the parameters characterized in Table 1. The number of data sets represented in each panel is limited to two for the readability of the plots.

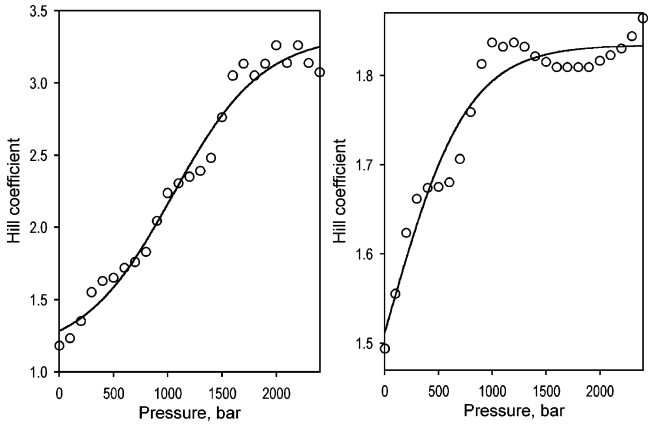

FIGURE 9: Effect of hydrostatic pressure on the cooperativity of interactions of CYP3A4 in solution with testosterone (left) and 1-PB (right). The values of the Hill coefficient at various pressures were obtained from the fitting of the data set shown in panels b and c of Figure 7 (right panels) to the Hill equation.

represented by two conformational states (R and P states) differing in the $\Delta V°$ of spin transition and substrate binding. The transition from the R to P state requires an important hydration of the protein so that the equilibrium between these states is displaced toward the P state by hydrostatic pressure. The binding of a non-allosteric substrate (BCT) to the R state is associated with a large positive volume change, whereas the volume changes upon the formation of the complexes of this state with allosteric substrates are considerably smaller. That may indicate that the binding of the first (effector) molecule of these substrates, which is silent in terms of substrate-induced spin shift, causes a conformational transition that facilitates the binding of the second substrate molecule. Although distinct from the R → P transition, this effector-induced rearrangement is able to displace the conformational equilibrium toward the P state, as seen in the case of interactions of CYP3A4 with testosterone (Table 2). The fact that the saturation of the enzyme with testosterone and 1-PB abolishes the effect of hydrostatic pressure on

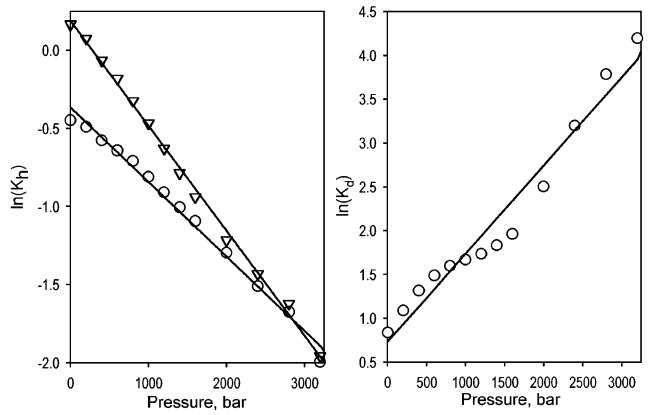

FIGURE 10: Effect of pressure on the parameters of the spin transition and substrate dissociation for the interactions of the heme domain of cytochrome P450 BM3 (BMP) with palmitic acid. The data represent the results of fitting of the data taken from our earlier publication (*31*). Pressure dependencies of the logarithms of constants of spin equilibrium $K_{h,free}$ (○) and $K_{h,S}$ (▽) are shown in the left panel. The right panel represents a similar plot for K_D. Solid lines show the linear approximation of the data sets.

substrate binding and spin equilibrium in the P state suggests that the interactions of this conformer of the enzyme with allosteric substrates result in a drastic decrease in the hydration and/or water accessibility of the heme pocket. It should be noted that, although the conformational equilibrium in CYP3A4 in solution and in CYP3A4ND is largely shifted toward the R state, a different situation may exist in the microsomal membrane, where the conformational equilibrium may be displaced by the interactions of CYP3A4 with NADPH-cytochrome P450 reductase and/or cytochrome b_5. This suggestion is consistent with our earlier observation that the barotropic behavior of the recombinant CYP3A4 in the membranes of yeast microsomes is similar to that reported here for the complexes of the P state of CYP3A4 with allosteric substrates in that hydrostatic pressure was unable to displace the spin equilibrium of the substrate-free or BCT-saturated enzyme completely to the low-spin state (*11*).

In addition to the discovery of a pressure-sensitive conformational equilibrium, the data obtained with monomeric CYP3A4ND confirm our earlier conclusion that the persistent conformational heterogeneity observed in CYP3A4 in solution (*1*, *11*) is due to the oligomerization of the enzyme. The change from oligomers of CYP3A4 in solution to the monomeric enzyme in Nanodiscs virtually abolishes this heterogeneity, as reflected in the pressure-induced P450 → P420 transition. Previously, we showed that the incorporation of the enzyme into Nanodiscs results in the disappearance of the middle phase of the three-exponential reduction kinetics with dithionite observed in oligomers (*1*). The relationship between the newly discovered pressure-sensitive conformational equilibrium in CYP3A4 and the persistent conformational heterogeneity of the enzyme in oligomers, which appears to be unaffected by pressure, remains unclear. An intriguing possibility is that the fraction of CYP3A4 in oligomers that is refractory to a pressure-induced P450 → P420 transition and is represented in the middle phase of the dithionite-dependent reduction may be excluded from the newly discovered R ↔ P equilibrium.

In summary, this study shows that pressure-perturbation experiments on CYP3A4−substrate interactions provide a valuable tool for the exploration of cooperativity. The

involvement of the large-range conformational transitions of CYP3A4 in the allosteric mechanisms demonstrated in this study is consistent with high conformational mobility of CYP3A4, as evidenced by recently resolved X-ray structures of the enzyme with erythromycin or ketoconazole (*6*). We believe that further studies combining the static pressure-perturbation or pressure-jump techniques with methods capable of detecting conformational transitions, such as fluorometric spectroscopy with the enzyme labeled with appropriate probes, NMR, or FT-IR spectroscopy, will provide a key for deeper understanding of the involvement of conformational malleability of CYP3A4 in the allosteric mechanisms.

ACKNOWLEDGMENT

We are grateful to Dr. Yelena V. Grinkova and Dr. Ilia G. Denisov (Department of Biochemistry, University of Illinois) for their help in the studies with Nanodiscs.

SUPPORTING INFORMATION AVAILABLE

Effect of hydrostatic pressure on tryptophan fluorescence of CYP3A4-containing Nanodiscs, pressure-induced changes in the fluorescence of DCVJ incorporated into Nanodiscs, effect of HPCD on the interactions of 1-PB and testosterone with CYP3A4, and effect of hydrostatic pressure on the fluorescence of complexes of 1-PB with HPCD. This material is available free of charge via the Internet at http://pubs.acs.org.

REFERENCES

1. Davydov, D. R., Fernando, H., Baas, B. J., Sligar, S. G., and Halpert, J. R. (2005) Kinetics of dithionite-dependent reduction of cytochrome P450 3A4: Heterogeneity of the enzyme caused by its oligomerization, *Biochemistry 44*, 13902−13913.
2. Tsalkova, T. N., Davydova, N. E., Halpert, J. R., and Davydov, D. R. (2007) Mechanism of interactions of α-naphthoflavone with cytochrome P450 3A4 explored with an engineered enzyme bearing a fluorescent probe, *Biochemistry 46*, 106−119.
3. Lampe, J. N., and Atkins, W. M. (2006) Time-resolved fluorescence studies of heterotropic ligand binding to cytochrome P450 3A4, *Biochemistry 45*, 12204−12215.
4. Scott, E. E., White, M. A., He, Y. A., Johnson, E. F., Stout, C. D., and Halpert, J. R. (2004) Structure of mammalian cytochrome P450 2B4 complexed with 4-(4-chlorophenyl)imidazole at 1.9-Å resolution: Insight into the range of P450 conformations and the coordination of redox partner binding, *J. Biol. Chem. 279*, 27294−27301.
5. Zhao, Y., White, M. A., Muralidhara, B. K., Sun, L., Halpert, J. R., and Stout, C. D. (2006) Structure of microsomal cytochrome P450 2B4 complexed with the antifungal drug bifonazole: Insight into P450 conformational plasticity and membrane interaction, *J. Biol. Chem. 281*, 5973−5981.
6. Ekroos, M., and Sjögren, T. (2006) Structural basis for ligand promiscuity in cytochrome P450 3A4, *Proc. Natl. Acad. Sci. U.S.A. 103*, 13684−13687.
7. Shou, M., Grogan, J., Mancewicz, J. A., Krausz, K. W., Gonzalez, F. J., Gelboin, H. V., and Korzekwa, K. R. (1994) Activation of CYP3A4: Evidence for the simultaneous binding of two substrates, *Biochemistry 33*, 6450−6455.
8. Korzekwa, K. R., Krishnamachary, N., Shou, M., Ogai, A., Parise, R. A., Rettie, A. E., Gonzalez, F. J., and Tracy, T. S. (1998) Evaluation of atypical cytochrome P450 kinetics with two-substrate models: Evidence that multiple substrates can simultaneously bind to cytochrome P450 active sites, *Biochemistry 37*, 4137−4147.
9. Ueng, Y. F., Kuwabara, T., Chun, Y. J., and Guengerich, F. P. (1997) Cooperativity in oxidations catalyzed by cytochrome P450 3A4, *Biochemistry 36*, 370−381.
10. Atkins, W. M., Wang, R. W., and Lu, A. Y. H. (2001) Allosteric behavior in cytochrome P450-dependent in vitro drug-drug interactions: A prospective based on conformational dynamics, *Chem. Res. Toxicol. 14*, 338−347.
11. Davydov, D. R., Halpert, J. R., Renaud, J. P., and Hui Bon Hoa, G. (2003) Conformational heterogeneity of cytochrome P450 3A4 revealed by high pressure spectroscopy, *Biochem. Biophys. Res. Commun. 312*, 121−130.
12. Davydov, D. R., Botchkareva, A. E., Kumar, S., He, Y. Q., and Halpert, J. R. (2004) An electrostatically driven conformational transition is involved in the mechanisms of substrate binding and cooperativity in cytochrome P450eryF, *Biochemistry 43*, 6475−6485.
13. Li, H., and Akasaka, K. (2006) Conformational fluctuations of proteins revealed by variable pressure NMR, *Biochim. Biophys. Acta 1764*, 331−345.
14. Occhipinti, E., Bec, N., Gambirasio, B., Baietta, G., Martelli, P. L., Casadio, R., Balny, C., Lange, R., and Tortora, P. (2006) Pressure and temperature as tools for investigating the role of individual non-covalent interactions in enzymatic reactions: *Sulfolobus solfataricus* carboxypeptidase as a model enzyme, *Biochim. Biophys. Acta 1764*, 563−572.
15. Kornblatt, J. A., and Kornblatt, M. J. (2002) The effects of osmotic and hydrostatic pressures on macromolecular systems, *Biochim. Biophys. Acta 1595*, 30−47.
16. Macgregor, R. B. (2002) The interactions of nucleic acids at elevated hydrostatic pressure, *Biochim. Biophys. Acta 1595*, 266−276.
17. Heremans, K., and Smeller, L. (1998) Protein structure and dynamics at high pressure, *Biochim. Biophys. Acta 1386*, 353−370.
18. Robinson, C. R., and Sligar, S. G. (1994) Hydrostatic pressure reverses osmotic pressure effects on the specificity of EcoRI-DNA interactions, *Biochemistry 33*, 3787−3792.
19. Fisher, M. T., Scarlata, S. F., and Sligar, S. G. (1985) High-pressure investigations of cytochrome P-450 spin and substrate binding equilibria, *Arch. Biochem. Biophys. 1*, 456−463.
20. Hui Bon Hoa, G., and Marden, M. C. (1982) The pressure dependence of the spin equilibrium in camphor-bound ferric cytochrome P-450, *Eur. J. Biochem. 124*, 311−315.
21. Marden, M. C., and Hoa, G. H. (1987) P-450 binding to substrates camphor and linalool versus pressure, *Arch. Biochem. Biophys. 253*, 100−107.
22. Di Primo, C., Hui Bon Hoa, G., Douzou, P., and Sligar, S. G. (1992) Heme-pocket-hydration change during the inactivation of cytochrome P-450camphor by hydrostatic pressure, *Eur. J. Biochem. 2*, 583−508.
23. Hui Bon Hoa, G., Di Primo, C., Dondaine, I., Sligar, S. G., Gunsalus, I. C., and Douzou, P. (1989) Conformational changes of cytochromes P-450cam and P-450lin induced by high pressure, *Biochemistry 28*, 651−656.
24. Tschirret-Guth, R. A., Hui Bon Hoa, G., and Ortiz de Montellano, R. P. (1998) Pressure-induced deformation of the cytochrome P450cam active site, *J. Am. Chem. Soc. 120*, 3590−3596.
25. Davydov, D. R., Knyushko, T. V., and Hui Bon Hoa, G. (1992) High pressure induced inactivation of ferrous cytochrome P-450 LM2 (2B4) CO complex: Evidence for the presence of two conformers in the oligomer, *Biochem. Biophys. Res. Commun. 188*, 216−221.
26. Davydov, D. R., Deprez, E., Hui Bon Hoa, G., Knyushko, T. V., Kuznetsova, G. P., Koen, Y. M., and Archakov, A. I. (1995) High-pressure induced transitions in microsomal cytochrome P450 2B4 in solution: Evidence for conformational inhomogeneity in the oligomers, *Arch. Biochem. Biophys. 320*, 330−344.
27. Davydov, D. R., Petushkova, N. A., Archakov, A. I., and Hui Bon Hoa, G. (2000) Stabilization of P450 2B4 by its association with P450 1A2 revealed by high-pressure spectroscopy, *Biochem. Biophys. Res. Commun. 276*, 1005−1012.
28. Anzenbacher, P., Bec, N., Hudecek, J., Lange, R., and Anzenbacherova, E. (1998) High conformational stability of cytochrome P-450 1A2. Evidence from UV absorption spectra, *Collect. Czech. Chem. Commun. 63*, 441−448.
29. Bancel, F., Bec, N., Ebel, C., and Lange, R. (1997) A central role for water in the control of the spin state of cytochrome P-450-(scc), *Eur. J. Biochem. 250*, 276−285.
30. Anzenbacherova, E., Bec, N., Anzenbacher, P., Hudecek, J., Soucek, P., Jung, C., Munro, A. W., and Lange, R. (2000) Flexibility and stability of the structure of cytochromes P450 3A4 and BM-3, *Eur. J. Biochem. 267*, 2916−2920.

31. Davydov, D. R., Hui Bon Hoa, G., and Peterson, J. A. (1999) Dynamics of protein-bound water in the heme domain of P450BM3 studied by high-pressure spectroscopy: Comparison with P450cam and P450 2B4, *Biochemistry 38*, 751−761.
32. Mclean, M. A., Maves, S. A., Weiss, K. E., Krepich, S., and Sligar, S. G. (1998) Characterization of a cytochrome P450 from the acidothermophilic archaea *Sulfolobus solfataricus*, *Biochem. Biophys. Res. Commun. 252*, 166−172.
33. Tschirret-Guth, R. A., Koo, L. S., Hoa, G. H. B., and de Montellano, P. R. O. (2001) Reversible pressure deformation of a thermophilic cytochrome P450 enzyme (CYP119) and its active-site mutants, *J. Am. Chem. Soc. 123*, 3412−3417.
34. Di Primo, C., Deprez, E., Hui Bon Hoa, G., and Douzou, P. (1995) Antagonistic effects of hydrostatic pressure and osmotic pressure on cytochrome P-450(cam) spin transition, *Biophys. J. 68*, 2056−2061.
35. Di Primo, C., Hui Bon Hoa, G., Douzou, P., and Sligar, S. (1990) Effect of the tyrosine 96 hydrogen bond on the inactivation of cytochrome P-450cam induced by hydrostatic pressure, *Eur. J. Biochem. 193*, 383−386.
36. Baas, B. J., Denisov, I. G., and Sligar, S. G. (2004) Homotropic cooperativity of monomeric cytochrome P450 3A4 in a nanoscale native bilayer environment, *Arch. Biochem. Biophys. 430*, 218−228.
37. Renaud, J. P., Davydov, D. R., Heirwegh, K. P. M., Mansuy, D., and Hui Bon Hoa, G. (1996) Thermodynamic studies of substrate binding and spin transitions in human cytochrome P450 3A4 expressed in yeast microsomes, *Biochem. J. 319*, 675−681.
38. Fernando, H., Halpert, J. R., and Davydov, D. R. (2006) Resolution of multiple substrate binding sites in cytochrome P450 3A4: The stoichiometry of the enzyme-substrate complexes probed by FRET and Job's titration, *Biochemistry 45*, 4199−4209.
39. Hui Bon Hoa, G., McLean, M. A., and Sligar, S. G. (2002) High pressure, a tool for exploring heme protein active sites, *Biochim. Biophys. Acta 1595*, 297−308.
40. Weber, G. (1991) *Protein Interactions*, Chapman and Hall, New York.
41. Kung, C. E., and Reed, J. K. (1986) Microviscosity measurements of phospholipid bilayers using fluorescent dyes that undergo torsional relaxation, *Biochemistry 25*, 6114−6121.
42. Denisov, I. G., Baas, B. J., Grinkova, Y. V., and Sligar, S. G. (2007) Cooperativity in P450 CYP3A4: Linkages in substrate binding, spin state, uncoupling and product formation, *J. Biol. Chem. 282*, 7066−7076.
43. Segel, I. H. (1975) *Enzyme Kinetics: Behavior and Analysis of Rapid Equilibrium and Steady-State Enzyme Systems*, Wiley-Interscience, New York.

BI602400Y